

Uncharged Water-Soluble Co(II)–Porphyrin: A Receptor for Aromatic α -Amino Acids

Nicola Angelini,[†] Norberto Micali,[†] Placido Mineo,^{*,‡} Emilio Scamporrino,[§] Valentina Villari,[†] and Daniele Vitalini[‡]

CNR–Istituto per i Processi Chimico-Fisici, sez. Messina, Via La Farina 237, I-98123 Messina, Italy,
CNR–Istituto di Chimica e Tecnologia dei Polimeri, Viale Andrea Doria 6, I-95125 Catania, Italy, and
Dipartimento di Scienze Chimiche, Università di Catania, Viale A. Doria 6, I-95125 Catania, Italy

Received: May 9, 2005; In Final Form: August 4, 2005

Changes in the UV–vis spectra and induced circular dichroism (ICD) signals observed, in correspondence with the porphyrin Soret region, for aqueous solutions of achiral 5,10,15,20-tetrakis[*p*-(ω -methoxy poly(oxyethylene))phenyl]porphyrin cobalt (II) (Co–P) and aromatic α -L-amino acids (Trp and Phe) give direct evidence for the coordination between the Co–P and amino acids. Considering that Co–P, besides the Co atom (one-fixation-point system), does not contain in the molecule active ligand groups and that no ICD signals have been observed in the case of Co–P/Ala, it has been concluded that hydrophobic interactions or stacking interactions between the aromatic rings of the porphyrin and those of Trp or Phe, acting as further amino acid (AA) fixation points, can strongly reduce the mobility of the chiral guest, thus permitting the generation of ICD signals. The effects of changes of both pH (in the range 2–9) and amino acid structure on the ICD phenomenon have also been investigated. In particular, the following have been observed: (i) strong ICD signals for all of the Co–P/*N*-acetyl amino acid aqueous solutions at pH 7, (ii) an unexpected ICD band with a bisignate form for the Co–P/Ala solution at pH 9 after long aging, and (iii) an opposite ICD signal when α -D-Phe and α -D-Trp enantiomers have been used. The data reported in this paper show how the binding mechanism between receptor and AAs changes by modulating properly the pH or the molecular structures and indicate that in these aqueous solutions the coordination Co–N is not the fundamental mechanism giving rise to the formation of the complexes and that the binding can be driven by hydrophobic interactions. These occurrences, through the analysis of the spectroscopic response (and, in particular, the form of the ICD band), can allow the recognition of AAs.

Introduction

Recent advanced research has led to the development of a large variety of smart nanostructures, possessing well-defined physicochemical properties, able to behave (just like smart molecules) as chemical and biological sensors, changing structure and/or properties in a measurable, reproducible and reversible manner in response to an appropriate external stimulus.^{1–7}

In the biomedical field, specific research has been devoted to the development of water-soluble molecules capable of selective analyte recognition for the diagnosis of biochemical anomalies or for the development of new pharmacological techniques. In this ambit, because of their vital role played in biological processes, metal porphyrins seem to be ideal candidates; as a consequence, recently, they have been studied for their ability to be molecular receptors of amino acids, polypeptides, or DNA (since metal porphyrin derivatives can provide recognition sites through the metal ion and/or the active functional groups in peripheral positions),^{8–12} in the treatment of the transmissible spongiform encephalopathy^{13,14} (inhibiting the formation of a protease-resistant protein), and in the localization and photodynamic therapy of tumors^{15–19} [because of both their strong affinity for neoplastic cells (“molecular finders”) and selective photo-oxidation by laser treatments].

In many of these studies, the porphyrin insolubility in aqueous media has been overcome by the introduction of ionic groups (pyridinium salts, carboxylate, sulfonate units, etc.) in peripheral molecular positions.^{20–22} However, although the presence of the free charges does not seem to modify the ligand properties of the porphyrin, in some cases (as an example, the crossing through cellular membranes), the possibility of undesirable effects with respect to the uncharged species cannot be excluded.²³

Consequently, our research^{24–27} has been directed to the design, synthesis, and characterization of new porphyrin derivatives (and their metal complexes) in which the presence of uncharged hydrophilic and biocompatible poly(ethylene glycol) units, bound to the meso porphyrin positions, makes these molecules hydrosoluble.

The data reported in the present paper are concerned with the modification of the spectroscopic properties (nuclear magnetic resonance, UV–visible absorption and circular dichroism) of a symmetric 5,10,15,20-tetrakis[*p*-(ω -methoxy poly(oxyethylene))phenyl]porphyrin cobalt(II) (Co–P) upon treatment with aliphatic and aromatic α -L-amino acids (AAs) in aqueous solutions. In particular, since the Co–P is an achiral product, the appearance of induced circular dichroism (ICD) signals in correspondence with the porphyrin Soret region constitutes direct evidence for the interaction between Co–P and aromatic amino acids to form chiral complexes.

With the aim of understanding in detail the character of interactions giving rise to the complex and what environmental

* Corresponding author. E-mail: gmineo@unict.it.

[†] CNR–Istituto per i Processi Chimico-Fisici.

[‡] CNR–Istituto di Chimica e Tecnologia dei Polimeri.

[§] Università di Catania.

factors can affect the binding sites, both the amino acid structure (*N*-acetyl-AA derivatives) and pH (in the range 2–9) have been changed. The appearance or disappearance of the ICD band, as well as its form depending on pH and amino acid structure, constitutes a fundamental key for exploiting this porphyrin as a receptor in recognition processes. All the experimental findings reported in the present paper allowed us to deduce that in aqueous solutions the Co–N coordination bond does not play a main role in the binding mechanism with AAs.

Experimental Section

UV–Visible Spectrophotometric Analysis. UV–visible (UV–vis) spectra were recorded on a Shimadzu model 1601 spectrophotometer at room temperature, using H₂O at different pHs as solvent.

MALDI-TOF Mass Spectrometric Analysis. The matrix-assisted laser desorption/ionization time-of-flight (MALDI-TOF) mass spectra were acquired by a Voyager DE-STR (PerSeptive Biosystem) using a simultaneous delay extraction procedure (20 kV applied after 233 ns with a potential gradient of 2545 V/mm and a wire voltage of 200 V) and detection in reflection mode. The instrument was equipped with a nitrogen laser (emission at 337 nm for 3 ns) and a flash AD converter (time base 2 ns). *trans*-3-Indoleacrylic acid was used as a matrix; the mass spectrometer calibration was performed as reported in previous cases,²⁸ and the average molecular masses were determined using a Grams/386 program (by PerSeptive Biosystem) applied on spectra corrected for the offset and the baseline according to our method.²⁹

¹H NMR and ¹³C NMR Analysis. ¹H NMR and ¹³C NMR spectra were acquired on an AC 200 F Bruker spectrometer interfaced with an Aspect 3000 computer, using the Bruker DISR 90 acquisition software. Samples were dissolved in CD₂-Cl₂ or in DMF-*d*₇ and the signal chemical shifts expressed in parts per million by comparison with the signal of tetramethylsilane (TMS) used as an internal standard. The DEPT 135° ¹³C spectra were acquired with the Bruker microprogram DEPT.AU. For aqueous solutions, the samples were dissolved in D₂O (at pH 9 by deuterated Borax buffer) and the chemical shifts expressed in parts per million by comparison with the signal of TMS used as an internal standard (coaxial insert).

Circular Dichroism Analysis. The circular dichroism spectra were recorded on a JASCO J-500A spectropolarimeter, with a 150 W xenon lamp. The apparatus was fully homemade and controlled by a PC computer. The ellipticity, $\theta \propto \epsilon_L - \epsilon_R$, was obtained by calibrating the instrument with a 0.06% aqueous solution of *d*-10-camporsulfonate. The measurements, corrected for the contribution from the cell and solvent, were performed at a constant temperature ($T = 22 \pm 0.1$ °C).

Materials. L- and D-Amino acids (AAs, Kit No. LAA-21) and their *N*-acetyl derivatives were obtained from Sigma Chemical Company. To facilitate the host/guest interaction between AAs and porphyrin, in all of the porphyrin/AA mixtures (except for the NMR experiments), the AAs were present in excess (in particular, a 2:1 molar ratio for the NMR analysis, 1:10 and 1:100 molar ratios for the UV–vis measurements, and a 1:100 molar ratio for the circular dichroism measurements). The metal porphyrin derivative concentration (see Figure 1 for the chemical structure) was 46 μM for all of the measurements. The measurements were performed on freshly prepared solutions (within 2 h) at pH 2, 7, and 9.

5,10,15,20-tetrakis[*p*-[ω-methoxy poly(oxyethylene)]phenyl]-porphyrin (H₂–P), having an average molecular mass of 3600 Da with a narrow polydispersity ($M_w/M_n = 1.01$), was prepared

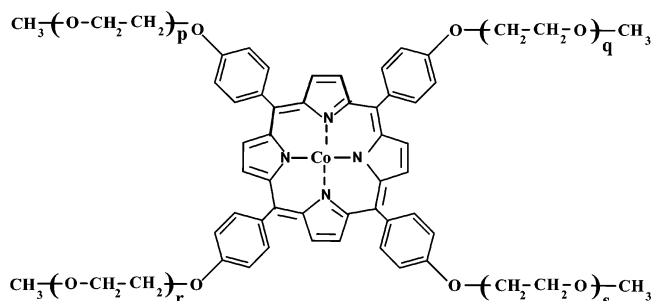


Figure 1. Chemical structure of 5,10,15,20-tetrakis[*p*-[ω-methoxy poly(oxyethylene)]phenyl]porphyrin cobalt(II).

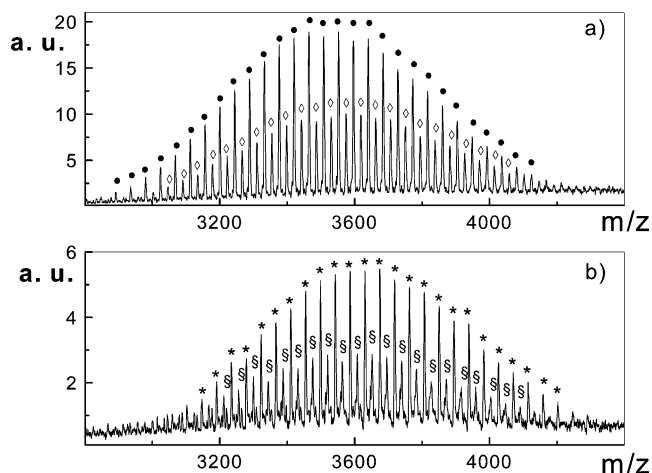


Figure 2. MALDI-TOF mass spectra of (a) H₂–P [consisting of two families of peaks due to species cationized by H⁺ (at m/z 2891 + $n44$, ●) and Na⁺ (at m/z 2913 + $n44$, ◇)] and (b) Co(II)–P [consisting of two families of peaks corresponding to species cationized by H⁺ (at m/z 2948 + $n44$, §) and Na⁺ (at m/z 2970 + $n44$, *)].

by reaction between tetrakis(*p*-hydroxyphenyl)porphyrin (obtained from pyrrole and *p*-acetoxybenzaldehyde in boiling propionic acid³⁰) and chlorinated poly(ethyleneglycol)methyl ether [PEGMEC, formed by reaction of poly(ethyleneglycol)-methyl ether with thionyl chloride in tetrahydrofuran (THF)] having an average molecular mass of 750 Da.²⁴

In a 10 mL flask, 1.07 g of PEGMEC-750 (about 1.43 mmol) was dissolved in 6 mL of a H₂O/THF (1:1) solution; after the addition of 0.12 g of tetrakis(*p*-hydroxyphenyl)porphyrin (0.177 mmol, half of the required stoichiometric quantity) dissolved in 1.42 mL of a 0.5 M NaOH aqueous solution, the mixture was refluxed for 24 h. Then, 1.42 mL of 0.5 M NaOH and 1.5 mL of THF were further added and the solution was continuously refluxed. After 24 h, the reaction was stopped by the addition of CH₃COOH, dried under vacuum and the residue, dissolved in CHCl₃, and fractionated by column chromatography using silica gel as the stationary phase and a solution of CHCl₃/C₂H₅OH/N(C₂H₅)₃ (96.5:2.0:1.5) as the eluant. As indicated by MALDI-TOF analysis, the first compound eluted from the column was the H₂–P (Figure 2a), which was collected with a yield of about 30% with respect to the initial porphyrin amount.

The chemical structure of the H₂–P was also determined by NMR spectroscopy; the ¹H and ¹³C NMR signal attributions are reported in the following. ¹H NMR: a singlet at 8.899 ppm (8 H, C–H pyrrole protons), two doublets at 8.131 ppm ($J = 8.6$ Hz; 8 H, C–H phenyl protons γ with respect to the phenolic oxygen) and at 7.325 ppm ($J = 8.6$ Hz; 8 H, C–H phenyl protons β with respect to the phenolic oxygen), and a singlet at –2.803 ppm (2 H, N–H pyrrole protons). The signals due to the PEG arms of the porphyrin present: two triplets centered

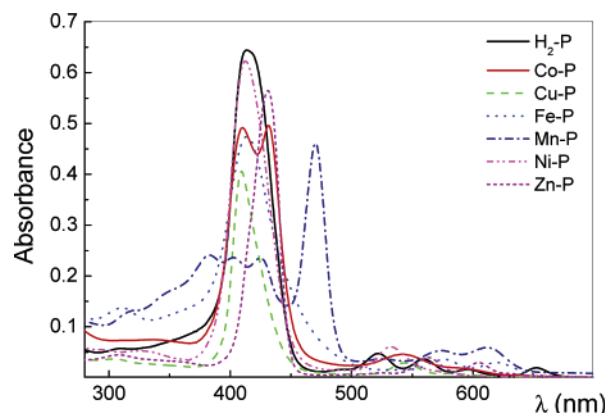


Figure 3. UV-vis spectra of H_2 -P and of its different metal derivatives.

at 4.419 and 4.016 ppm (for a total of 16 H, CH_2 groups in the α and β positions, respectively, with respect to the phenolic oxygen), an unresolved multiplet between 3.85 and 3.43 ppm (about 230 H, the other methylene groups of the PEG), and a few singlets between 3.33 and 3.30 ppm (12 H, the CH_3 terminal groups of the branches).

^{13}C NMR: 159.119, 134.973, and 120.172 ppm (quaternary carbons), 135.971 and 113.190 ppm (phenyl tertiary carbons in the γ and β positions, respectively, with respect to the phenolic oxygen), 131.375 ppm (broad signal of pyrrole tertiary carbons), 72.2 \div 68.2 ppm (a few peaks due to PEG secondary carbons), and 68.202 ppm (terminal PEG methyl groups). The signal corresponding to the fourth quaternary carbon, normally present at about 146.5 ppm,³¹ is practically absent in this case, probably because of a longer relaxation time of this carbon atom with respect to the other ones; to ascertain its presence, a new ^{13}C NMR experiment was carried out by dissolving the sample in deuterated dimethylformamide (DMF) and acquiring the spectrum at 80 °C. Under these conditions, not only the missing quaternary carbon signal appears at 147.527 ppm, but also the broad peak due to the tertiary carbons of pyrrole at 131.521 ppm (little shifted with respect to the previous value because of the change of solvent and temperature) became sharper, indicating that, at this temperature, the relaxation times of the aromatic carbons are shorter.

The metal 5,10,15,20-tetrakis[*p*-[ω -methoxy poly(oxyethylene)]phenyl]porphyrins were obtained as previously described,²⁶ and as an example, the synthesis of the Co(II) derivative (Figure 1) is reported here. The H_2 -P and the teen excesses fold of cobalt(II) acetate were dissolved in pyridine, refluxed for 4 h in a N_2 atmosphere, and then evaporated under vacuum. Pure 5,10,15,20-tetrakis[*p*-[ω -methoxy poly(oxyethylene)]phenyl]porphyrin cobalt(II) [in which a cobalt(II) ion is substituted for the two hydrogen atoms of the porphyrin core] was obtained by column chromatography separation, using silica gel as the stationary phase and a solution of $CHCl_3/C_2H_5OH/N(C_2H_5)_3$ (96.5:2.0:1.5) as the eluant; its MALDI-TOF mass spectrum is shown in Figure 2b.

Due to the paramagnetic property of cobalt(II), it was not possible to record appreciable 1H and ^{13}C NMR spectra of this compound (both in fresh and aged solutions).

Results and Discussion

Soret regions of the UV-visible spectra of some aqueous solutions of pure 5,10,15,20-tetrakis[*p*-[ω -methoxy poly(oxyethylene)]phenyl]porphyrin (H_2 -P) (solid line) and its Mn, Fe, Co, Ni, Cu, and Zn metal derivatives (Me-P) are shown in Figure 3.

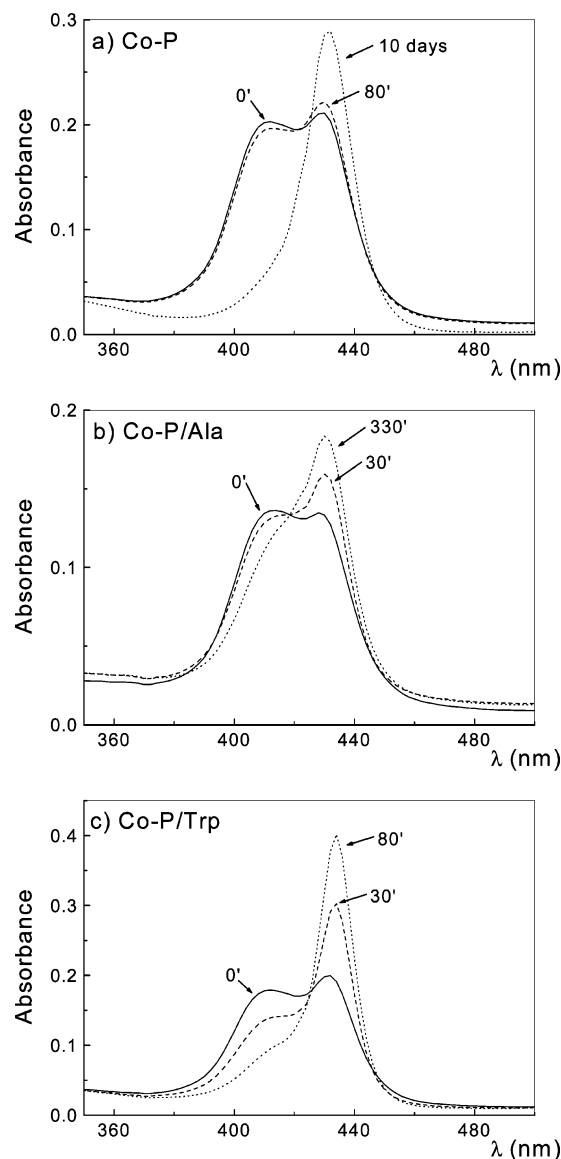


Figure 4. UV-vis spectral modifications induced by aging on buffered solutions at pH 9: (a) Co-P; (b) Co-P/Ala; (c) Co-P/Trp.

As previously reported for similar compounds,^{32–34} depending on the metal inserted in the porphyrin core, relevant changes in the position (typically a red or blue shift), shape (a splitting in more signals), and/or intensity of the Soret band are observed. Also, the spectral regions of the Q-bands are strongly affected, with the disappearance of two bands and a shift of the remaining signals; however, since these bands are much less intense than the Soret signal, they will be neglected in the following discussion.

As an example, the Soret region of a freshly prepared aqueous solution of Co-P (solid line in Figure 4a) can be considered: in contrast with what happens in organic solvents, the absorption spectrum of Co-P in this region is constituted by two overlapped signals of comparable intensity, having λ_{max} values at about 410 and 430 nm; as previously reported for similar cases,^{35,36} they can be ascribed to the equilibrium between Co-P and its complexed species having a different number of ligands (H_2O , OH^- , and/or borate ions) bound to the metal atom in axial positions with respect to the porphyrin plane. The comparison of this spectrum with those recorded after 80 min or 10 days of aging, reported in Figure 4a, points out the gradual disappearance of the signal at 410 nm and the corresponding increment of the band at 432 nm, indicating that the equilibrium

is time dependent with a complete red shift of the signal after about 10 days of aging.

This spectral shift can be explained if we consider the Soret band in metalloporphyrin optical spectra as $\pi-\pi^*$ excitations localized on the porphyrato macrocycle, from the two highest occupied porphyrin π -molecular orbitals (a_{2u} and a_{1u} in D_{4h} symmetry) to the lowest pair of unoccupied orbitals (e.g., in D_{4h} symmetry).^{37–39} By this model, the spectral shift observed in the presence of an axial ligand is a consequence of the variation of the a_{2u} orbital energy, caused by interactions with the central metal. The a_{1u} orbital has nodes at the pyrrole nitrogen, so that it should be much less influenced by perturbations due to the central metal.⁴⁰

The metal porphyrin behavior as a receptor of amino acids (AAs), as a function of the metal coordinated, has been tested by examining the UV–vis spectra of aqueous solutions at pH 9 (for Borax buffer) of several Me–P derivatives with some aliphatic and aromatic α -L-AAs [alanine (Ala), phenylalanine (Phe), and tryptophan (Trp); molar ratio 1:10], but remarkably, an appreciable spectral modification appeared only in the case of Co–P.

The comparison of the spectral modifications induced by aging on the UV–vis spectra of Co–P/Ala (Figure 4b) and Co–P/Trp (Figure 4c) with respect to those observed in the case of Co–P (Figure 4a) is indicative of a more kinetically favorable axial coordination of the AA molecules to the Co atom with respect to water or other ionic ligands.^{36b} An easier coordination of Trp and Phe (which behaves similarly to Trp; spectra omitted for brevity) with respect to Ala also results.

The observed UV–vis modifications are indicative of Co–P/AA interaction, which could take place through the coordination bond between the metal atom of the porphyrin (host) and the amine group of the AA (guest), as reported by some authors.^{10,41,42}

This behavior is also supported by NMR analysis: some changes in the ^1H NMR spectra of D_2O solutions of Co–P/AAs, with respect to those of pure AAs, are certainly in agreement with the complex formation between metal porphyrins and amino acid molecules. As an example, the signals of the aromatic hydrogens (between 7 and 5.8 ppm) of the ^1H NMR spectrum of pure tyrosine (Tyr, curve a) are compared, in Figure 5, with those of its mixtures with free porphyrin ($\text{H}_2\text{P/Tyr}$, curve b) and metal porphyrins (Ni–P/Tyr, curve c, and Co–P/Tyr, curve d). Weak interactions between Tyr and both H_2P and Ni–P (curves b and c) are evidenced by little shifts of the corresponding signals; on the contrary, remarkable alterations are observed in the case of Co–P/Tyr in which new signals are present in the spectrum, at about 6.05, 6.37, and 6.75 ppm, and both new and old peaks are considerably broadened. Similar results, symptomatic of an intense interaction between AA and Co–P, have also been obtained using Phe and Trp instead of Tyr.

The interaction between the Co–P and AAs was further investigated by circular dichroism (CD) analysis, which gives clearer and more resolute evidence than UV and NMR analysis on the binding phenomenon. Figure 6 shows the UV–vis (Figure 6a) and CD (Figure 6b) spectra of the aqueous solutions, at pH 7, of Co–P and of its mixtures with Ala, Phe, and Trp. As expected, considering the symmetric structure of Co–P, no CD signals appear in the spectrum of Figure 6b(I). Also, the spectrum of Co–P/Ala [Figure 6b(II)] does not show significant peaks, whereas, in the cases of Co–P/Phe and Co–P/Trp [Figure 6b(III) and (IV)], the clear negative CD signals, in

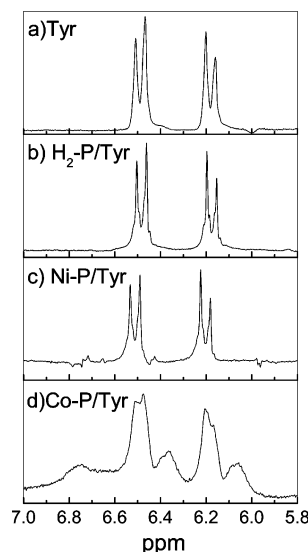


Figure 5. Signals of aromatic hydrogens (between 7.0 and 5.8 ppm) of ^1H NMR spectra of pure tyrosine (Tyr, curve a) and of its mixtures with free porphyrin ($\text{H}_2\text{P/Tyr}$, curve b) and Ni or Co metal porphyrins [Ni–P/Tyr (curve c) and Co–P/Tyr (curve d)].

correspondence with the Soret band at 432 nm, give direct evidence for the coordination between the Co–P and Phe or Trp.

Generally, the binding of chiral AAs to porphyrins gives rise to the asymmetric perturbation of the porphyrin electric transition moment; as a consequence, the chiral complex so obtained generates an induced CD (ICD) phenomenon. It is known that, in the presence of chiral AAs bound to a metal porphyrin by “two-point fixation” (i.e., besides the metal atom, a peripheral active group, by a hydrogen bond with the AA carbonyl group in organic solvents or by electrostatic interactions of the carboxyl group in aqueous solution), ICD signals are displayed.^{9,43–47} Analogous results have been also obtained for some complexes having “one-point fixation” (i.e., the metal atom, coordination through the AA amine group), when an additional molecular interaction reduces the mobility of the AA.^{9,48}

Thus, considering the spectral UV–vis modifications shown in Figures 4b and 6a(II) in the case of Co–P/Ala, the absence of a significant ICD signal (under our experimental conditions) could be explained by considering that the porphyrin does not present peripheral donor groups suitable for an additional bond, beyond that between the Ala amine group and the Co atom. On the contrary, a stacking interaction between the aromatic rings of the porphyrin and those of Trp or Phe, acting as a further AA fixation point, can strongly reduce the mobility of the chiral guest and can cause the ICD observed in Figure 6b(III) and (IV).

Because no ICD signal is observed for aqueous $\text{H}_2\text{P/AA}$ mixtures (spectra omitted for brevity), the Co atom is surely involved in the formation of the complex.

As further evidence for the chirality induction on Co–P (which excludes artifacts from eventual linear dichroism contribution), the spectra of aqueous solutions of Co–P with α -D-Phe and α -D-Trp exhibit an opposite ICD signal (showing a positive Cotton effect; spectra omitted for brevity) with respect to the α -L-enantiomers.

The effect of pH changes on the ICD of Co–P/AAs aqueous solutions has also been investigated in order to understand how the chemical environment can act on the coordination sites affecting the Co–P/AAs interactions. Both the UV–visible and ICD spectra of the Co–P/Phe at pH 2, 7, and 9 are shown in

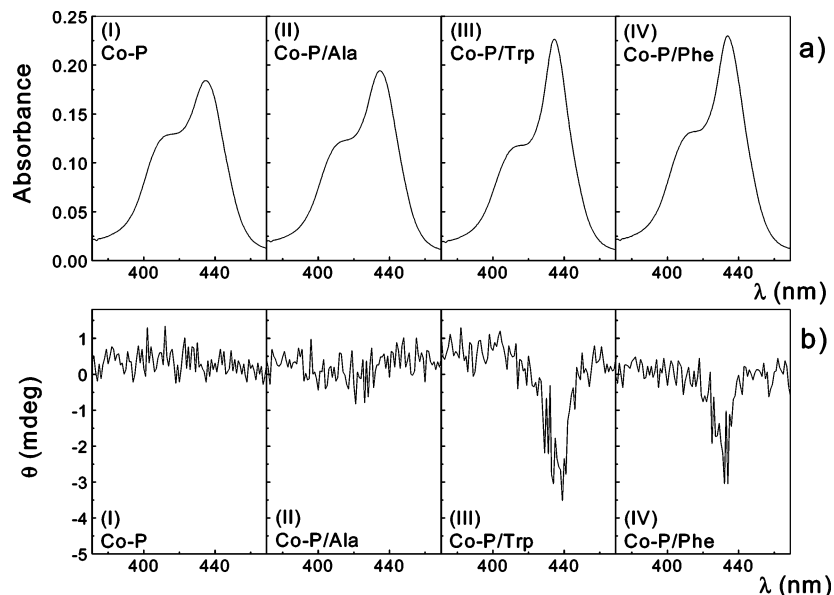


Figure 6. (a) UV–vis and (b) CD spectra of aqueous solutions at pH 7 of Co–P and of its mixtures with different amino acids.

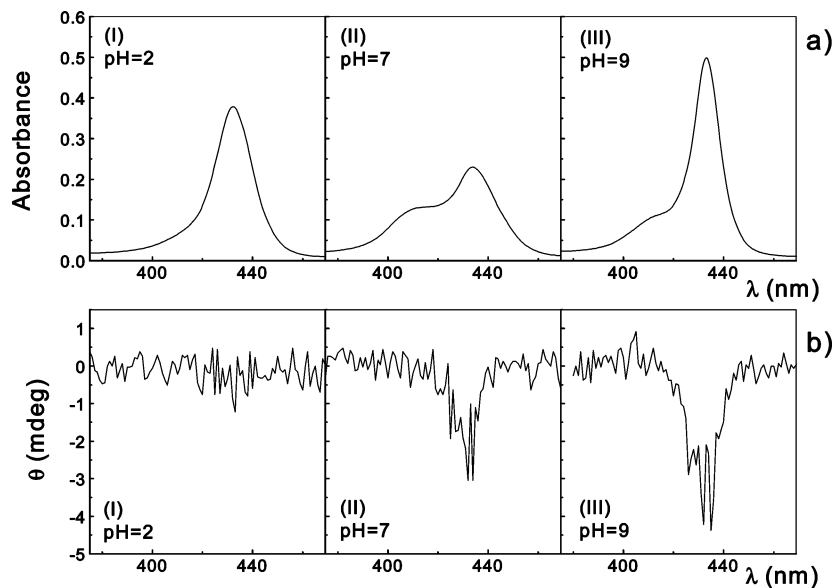


Figure 7. (a) UV–vis and (b) CD spectra of aqueous solutions of Co–P/Phe at different pH values.

Figure 7. It can be observed that the intensity of the UV–vis band at 432 nm decreases upon going from pH 9 [Figure 7a(III)] to pH 7 [Figure 7a(II)] but increases again at pH 2 where, on the contrary, the band at 410 nm almost disappears [Figure 7a(I)]. Also, the ICD peak at pH 7 [Figure 7b(II)] is lower than that at pH 9 [Figure 7b(III)] but, unexpectedly, it totally disappears at pH 2 [Figure 7b(I)] (similar results have been obtained in the case of Trp).

These data can be rationalized considering the effect of the pH change on the equilibrium among the different AA species in aqueous solution ($^+H_3N-CHR-COOH \rightleftharpoons ^+H_3N-CHR-COO^- \rightleftharpoons H_2N-CHR-COO^-$). Passing from pH 9 to pH 7 (value near the AA isoelectric point, about pH 6), the amine group gradually becomes less available for the Co coordination so that the intensities of both the UV–vis band at 432 nm and the corresponding ICD signal decrease.

Because the amine groups are totally protonated at pH 2, the complexation of the AA is prevented and no ICD appears. In this case, the apparently anomalous increase of the UV–vis band at 432 nm can be explained considering that, having used HCl to reach pH 2, the guest chiral AA molecules are substituted

by the achiral Cl^- ions; as a consequence, no ICD appears, whereas the Soret band is always red shifted for the metal coordination.

To further investigate the role played by the Co–N coordination in the Co–P/AA complex formation, aqueous solutions of Co–P and *N*-acetyl-L-amino acid (*N*-AcAA) derivatives were examined. Summarizing the results, no ICD signals have been detected at pH 9 either in NaOH or in Borax buffer, but surprisingly, a clear ICD signal has been observed for all *N*-AcAAs at pH 7. As an example, it can be noticed that the Co–P/*N*-acetyl-L-phenylalanine complex (Co–P/*N*-AcPhe) shows an ICD signal [Figure 8b(II)] stronger than that of the corresponding Co–P/Phe [Figure 8b(I)].

From these findings, it is clear that, in aqueous solutions, the coordination bond Co(host)–N(guest) does not play a fundamental role; the binding mechanism between Co–P and AAs can involve more complex interactions, as, for example, a delicate balance between different interaction strengths which also depend on the competition with the solvent. However, considering that electrostatic interactions are absent and that aromatic amino acids show a preferential interaction, hydro-

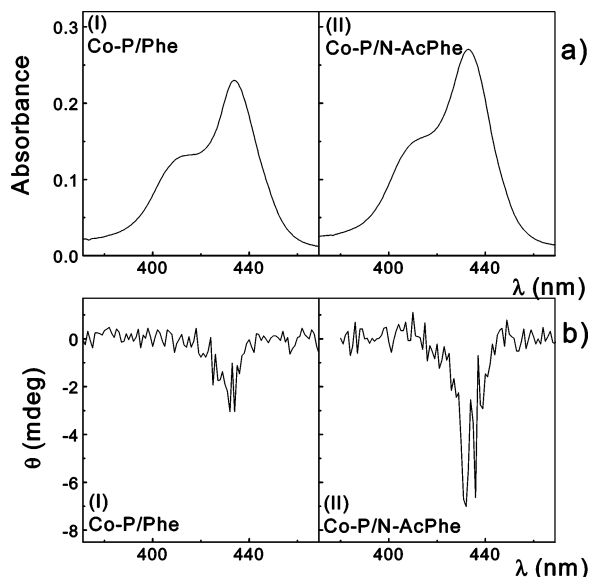


Figure 8. (a) UV-vis and (b) CD spectra of aqueous solutions at pH 7 of Co-P/Phe and Co-P/N-AcPhe.

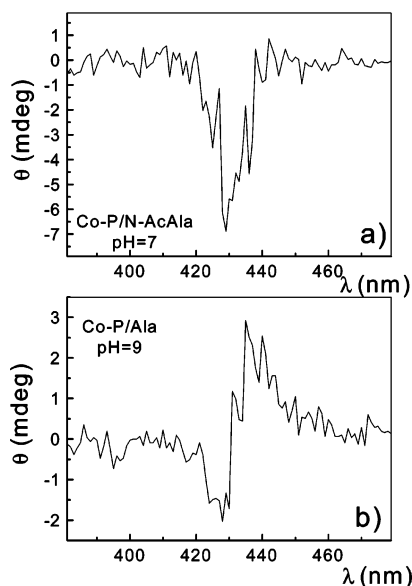


Figure 9. ICD signals of aqueous solutions of (a) Co-P/N-AcAla (at pH 7) and (b) aged Co-P/Ala (at pH 9).

phobically driven and/or stacking interactions could be addressed as the main cause of the formation of Co-P/AA complexes in aqueous solutions.

Moreover, while Co-P/Ala solution at pH 7 does not exhibit significant ICD signals [see Figure 6b(II)], a negative ICD signal has been recorded for a solution of Co-P/N-AcAla (see Figure 9a), indicating that this latter system, lacking aromatic rings, behaves like Co-P/N-AcPhe and Co-P/N-AcTrp. As a hypothesis, this result can be rationalized considering that the flat amide group (coordinated to the Co atom) introduces steric effects and/or hydrophobic contributions which, hindering structural rotations, stabilize the complex.

An unexpected ICD signal (shown in Figure 9b) has been observed for an aged 48 h Co-P/Ala aqueous solution at pH 9 [both in NaOH and in Borax buffer; for comparison, see also the Co-P/Ala trace in Figure 6b(II)]. Remarkably, this ICD band, different from those obtained for the aromatic amino acids, shows a split type Cotton effect.

From a general point of view, the split Cotton effect is observed when identical or nearly identical chromophores,

having a high extinction coefficient, come into contact so that their electric transition moments couple very efficiently. This coupling is known as exciton coupling, and it yields a bisignate CD curve. For the ICD phenomenon, however, the coupling occurs between different molecules and, therefore, between different transition moments so that the ICD band displays usually a peak or a trough. However, some authors^{48,49} found bisignate ICD in the absence of electronic communication between two chromophores, so that the split type ICD observed for the aged Co-P/Ala complex can be ascribed to different interaction mechanisms. In the case of the Co-P/Ala complex, the hypothesis that two Co-P come into close contact is strengthened considering previous results of time resolved fluorescence anisotropy.²⁷ It has been shown that the Co-P rotational correlation time on the aged Co-P/Ala is almost double in comparison with that of Co-P alone and larger than that of Co-P/Phe and Co-P/Trp. This result suggests that the bisignate ICD could be due to a kinetically slow process which could give rise to the formation of a Co-P/Ala/Co-P sandwich structure in which each alanine binds two Co-P molecules through its amine and carboxylate groups ($\text{H}_2\text{N}-\text{CHR}-\text{COO}^-$). This hypothesis is also supported by the disappearance of ICD signals for Co-P/Ala aqueous solution at pH 7 (near the isoelectric point of the AA), because of the reduced number of available COO^- binding sites. Probably, Co-P/Phe and Co-P/Trp do not give rise to similar bisignate ICD signals because a steric hindrance prevents the necessary close approach of two Co-P molecules to form the sandwich conformation. However, it has to be noticed that the coupling of two porphyrins gives rise, generally, to ICD signals much stronger than that observed in Figure 9b.

It is worth noting that, at pH 9 (both in Borax buffer and in NaOH), the binding occurs for all of the investigated AAs (even if the involved time scales are quite different), whereas it is prevented for all of the *N*-AcAAs. Probably, this feature has to be ascribed to the coordination competition of the *N*-AcAA derivatives with the stronger hydroxyl or Borax guest species.

Conclusions

UV-vis and NMR results suggest the presence of interaction phenomena between Co-P and AAs; in particular, UV-vis spectra show a more kinetically favorite axial coordination of AAs with the cobalt atom of the porphyrin and ^1H NMR spectra present remarkable alterations of the AA signals. More direct evidence of the binding mechanism comes from the circular dichroism measurements and, in particular, from the study of the ICD. Although the Co-P derivative studied here does not contain active ligand groups, except for the central metal atom (one fixation point), clear ICD signals have been observed in the aqueous solutions, at neutral pH, of Co-P/Phe and Co-P/Trp. The absence of ICD in the Co-P/Ala solution suggests that the stacking interactions between the aromatic rings of porphyrin and aromatic AAs act as a further fixing point (plane).

The appearance of an unexpected ICD band with a bisignate form, in the experiments with Ala at pH 9 (after aging), suggests the occurrence of a Co-P/Ala/Co-P sandwich structure, in which each Ala unit coordinates two Co-P molecules.

The Co-P solutions in the presence of the *N*-acetyl amino acid derivatives, both aromatic and aliphatic, display very similar ICD bands at pH 7, suggesting that in these aqueous solutions the coordination Co-N is not the fundamental mechanism giving rise to the formation of the complexes and that the binding can be driven by hydrophobic interactions. In this case, the induced chirality can be explained by considering that the

flat amide group, causing steric or hydrophobic effects, stabilizes the complex structure enough even in the absence of aromatic rings.

The results reported in this paper clearly show how the binding mechanism between receptor and AAs changes by modulating properly the pH or the molecular features. This occurrence, through the analysis of the spectroscopic response (and, in particular, the form and intensity of the ICD band), allows for the recognition of AAs.

Acknowledgment. Partial financial support from the Ministero Istruzione, Università e Ricerca, and CNR-Rome is gratefully acknowledged.

References and Notes

- (1) Pompa, P. P.; Biasco, A.; Cingolani, R.; Rinaldi, R.; Verbeet, M. Ph.; Canters, G. W. *Phys. Rev. E* **2004**, *69*, 032901/1–032901/4.
- (2) Czeslik, C.; Jansen, R.; Ballauff, M.; Wittemann, A.; Royer, C. A.; Gratton, E.; Hazlett, T. *Phys. Rev. E* **2004**, *69*, 021401/1–021401/9.
- (3) Caruso, F.; Caruso, R. A.; Mohwald, H. *Science* **1998**, *282*, 1111–1114.
- (4) Awawdeh, M. A.; Legako, J. A.; Harmon, H. J. *Sens. Actuators, B* **2003**, *91*, 227–230.
- (5) Robertson, A.; Shinkai, S. *Coord. Chem. Rev.* **2000**, *205*, 157–199.
- (6) Purrello, R.; Gurrieri, S.; Lauceri, R. *Coord. Chem. Rev.* **1999**, *190–192*, 683–706.
- (7) Purrello, R.; Raudino, A.; Scolaro, L.; Monsu, Loisi, A.; Bellacchio, E.; Lauceri, R. *J. Phys. Chem. B* **2000**, *104*, 10900–10908.
- (8) Aoyama, Y.; Yamagishi, A.; Asagawa, M.; Toi, H.; Ogoshi, H. *J. Am. Chem. Soc.* **1988**, *110*, 4076–4077.
- (9) Mizutani, T.; Wada, K.; Kitagawa, S. *J. Am. Chem. Soc.* **1999**, *121*, 11425–11431.
- (10) Mikros, E.; Gaudemer, F.; Gaudemer, A. *Inorg. Chem.* **1991**, *30*, 1806–1815.
- (11) Verchere-Beaur, C.; Mikros, E.; Perre-Fauvet, M.; Gaudemer, A. *J. Inorg. Biochem.* **1990**, *40*, 127–139.
- (12) Borovkov, V. V.; Lintuluoto, J. M.; Inoue, Y. *J. Am. Chem. Soc.* **2001**, *123*, 2979–2989.
- (13) Priola, S. A.; Raines, A.; Caughey, W. S. *Science* **2000**, *287*, 1503–1506.
- (14) Sternberg, E. D.; Dolphin, D.; Bruckner, C. *Tetrahedron* **1998**, *54*, 4151–4202.
- (15) Nyman, E. S.; Hynninen, P. H. *J. Photochem. Photobiol., B* **2004**, *73*, 1–28.
- (16) Jori, G. *J. Photochem. Photobiol., B* **1996**, *36*, 87–93.
- (17) Zenkevich, E.; Sagun, E.; Knyukshto, V.; Shulga, A.; Mironov, A.; Efremova, O.; Bonnett, R.; Songca, S. P.; Kassem, M. *J. Photochem. Photobiol., B* **1996**, *33*, 171–180.
- (18) Ris, H. B.; Krueger, T.; Giger, A.; Lim, C. K.; Stewart, J. C. M.; Althaus, U.; Altermatt, H. *J. Br. J. Cancer* **1999**, *79*, 1061–1066.
- (19) Aime, S.; Botta, M.; Gianolio, E.; Terreno, E. *Angew. Chem., Int. Ed.* **2000**, *39*, 747–750.
- (20) Anneheimherbelin, G.; Perreefauvet, M.; Gaudemer, A.; Helissey, P.; Giorgirenauld, S.; Gresh, N. *Tetrahedron Lett.* **1993**, *34*, 7263–7266.
- (21) Ci, Y. X.; Zheng, Y. G.; Tie, J. K.; Chang, W. B. *Anal. Chim. Acta* **1993**, *282*, 695–701.
- (22) Vercherebeaur, C.; Perreefauvet, M.; Tarnaud, E.; Anneheimherbelin, G.; Bone, N.; Gaudemer, A. *Tetrahedron* **1996**, *52*, 13589–13604.
- (23) Schneider, H. J.; Wang, M. X. *J. Org. Chem.* **1994**, *59*, 7473–7478.
- (24) Mineo, P.; Vitalini, D.; Scamporrino, E. *Macromol. Rapid Commun.* **2002**, *23*, 681–687.
- (25) Micali, N.; Villari, V.; Mineo, P.; Vitalini, D.; Scamporrino, E.; Crupi, V.; Majolino, D.; Migliardo, P.; Venuti, V. *J. Phys. Chem. B* **2003**, *107* (21), 5095–5100.
- (26) Mineo, P.; Scamporrino, E.; Vitalini, D. Consiglio Nazionale delle Ricerche; Università di Catania *Patent and Appl. No. MI2004A001135*.
- (27) Angelini, N.; Micali, N.; Villari, V.; Mineo, P.; Scamporrino, E.; Vitalini, D. *Phys. Rev. E* **2005**, *71*, 21915/1–21915/7.
- (28) Scamporrino, E.; Vitalini, D.; Mineo, P. *Macromolecules* **1996**, *29*, 5520–5528.
- (29) Scamporrino, E.; Vitalini, D.; Mineo, P. *Macromolecules* **1997**, *30*, 5285–5289; *Rapid Commun. Mass Spectrom.* **1999**, *13*, 2511–2517.
- (30) Little, R. G.; Anton, J. A.; Loach, P. A.; Ibers, J. A. *J. Heterocycl. Chem.* **1975**, *12*, 343–347.
- (31) Scamporrino, E.; Vitalini, D.; Mineo, P. *Macromolecules* **1999**, *32*, 60–69.
- (32) Liao, M. S.; Scheiner, S. J. *Chem. Phys.* **2002**, *117*, 205–219.
- (33) Wang, R.; Hoffman, B. M. *J. Am. Chem. Soc.* **1984**, *106*, 4235–4240.
- (34) Shelnutt, J. A.; Ortiz, V. J. *Phys. Chem.* **1985**, *89*, 4733–4739.
- (35) (a) Pasternack, R. F.; Francesconi, L.; Raff, D.; Spiro, E. *Inorg. Chem.* **1973**, *12*, 2606–2611. (b) Pasternack, R. F.; Cobb, M. A.; Sutin, N. *Inorg. Chem.* **1975**, *14*, 866.
- (36) Pasternack, R. F.; Spiro, E.; Teach, M. J. *Inorg. Nucl. Chem.* **1974**, *36*, 599–606.
- (37) Gouterman, M. *J. Mol. Spectrosc.* **1961**, *6*, 138–163.
- (38) Gouterman, M.; Wagniere, G. H.; Snyder, L. C. *J. Mol. Spectrosc.* **1963**, *11*, 108–127.
- (39) Spellane, P. J.; Gouterman, M.; Antigas, A.; Kim, S.; Liu, Y. C. *Inorg. Chem.* **1980**, *19*, 386–391.
- (40) Wang, R. M.-Y.; Hoffman, M. J. *J. Am. Chem. Soc.* **1984**, *106*, 4235–4240.
- (41) Walker, A. F. *J. Am. Chem. Soc.* **1973**, *95*, 1150–1153.
- (42) Sekota, M.; Nyokong, T. *Polyhedron* **1997**, *19*, 3279–3284.
- (43) Aoyama, Y.; Yamagishi, A.; Asagawa, M.; Toi, H.; Ogoshi, H. *J. Am. Chem. Soc.* **1988**, *110*, 4076–4077.
- (44) Borovkov, V. V.; Lintuluoto, J. M.; Hembury, G. A.; Sugiura, M.; Arakawa, R.; Inoue, Y. *J. Org. Chem.* **2003**, *68*, 7176–7192.
- (45) Ogoshi, H.; Mizutani, T. *Acc. Chem. Res.* **1998**, *31*, 81–89.
- (46) Huang, X.; Nakanishi, K.; Berova, N. *Chirality* **2000**, *12*, 237–255.
- (47) Borovkov, V. V.; Lintuluoto, J. M.; Inoue, Y. *J. Am. Chem. Soc.* **2001**, *123*, 2979–2989.
- (48) Mizutani, T.; Ema, T.; Yoshida, T.; Rennè, T.; Ogoshi, H. *Inorg. Chem.* **1994**, *33*, 3558–3566.
- (49) Balaz, M.; De Napoli, M.; Holmes, A. E.; Mammana, A.; Nakanishi, K.; Berova, N.; Purrello, R. *Angew. Chem.* **2005**, *117*, 4074–4077.